P2.57 PRECIPITATION STRUCTURE IN MIDLATITUDE CYCLONES

Paul R. Field[1]*, Robert Wood[2]
1. National Center for Atmospheric Research , Boulder, Colorado .
2. University of Washington, Seattle, Washington.

1. Introduction

Midlatitude, or extratropical, cyclones (hereafter referred to simply as cyclones) are an important component of the atmospheric general circulation due to their ability to redistribute large amounts of heat, moisture, and momentum. Cyclones are driven by temperature gradients between the warm subtropics and the cold polar regions and are the primary atmospheric conduit for poleward energy transfer in the midlatitudes. Their influence on weather and climate and their consequences for life have resulted in extensive study of these systems, and a rich literature concerning the synoptic nature of cyclones extends from the Norwegian conceptual model introduced by Bjerknes (1919) through to the recent review edited by Shapiro and Grønas (1999).

In this study we use reanalysis data to determine a cyclone-center-relative coordinate system into which various satellite data are transformed and then composited to provide a view of a cyclone from the perspective of the low pressure center.

We have approached this compositing exercise assuming the following two premises. *i) On average a cyclone will exhibit similar precipitation and cloud structure to another cyclone if the thermodynamic and mesoscale dynamical environments are comparable. ii) The thermodynamic and mesoscale dynamical environment for each cyclone can be categorized by two metrics that represent the mean atmospheric moisture and the mean cyclone strength.* It has been previously surmised that the structural properties of clouds and precipitation within cyclones are a response to both their mesoscale dynamics and thermodynamically environment (e.g. Norris and Iacobellis, 2005, Chang and Song 2006). The intention of this study is to show that much of the variation between the precipitation and cloud composites of cyclones, for example, seasonal variability can be understood quantitatively in terms of cyclone strength and atmospheric moisture. Understanding the change in cyclone cloudiness and precipitation with respect to these two metrics will allow us to quantitatively answer questions posed by studies that suggest mean cyclone strength and frequency are changing as a result of climate change.

This abstract is an abbreviated form of a paper submitted to the Journal of Climate: Field and Wood (2006).

* *Corresponding author address*: Paul R. Field NCAR, PO Box 3000, Boulder, CO 80307; e-mail: prfield@ucar.edu.

2. Data

2.1 AMSR-E

The Advanced Microwave Scanning Radiometer (AMSR-E), on the NASA Aqua sun-synchronous satellite, provides near complete coverage each day of several important parameters used in this study. For this study we use surface rain rate and column integrated water vapor estimates (WVP: water vapor path. Wentz, 1997; Wentz and Spencer, 1998) obtained from AMSR-E data (Version 5) provided by Remote Sensing Systems (RSS). Additional information regarding these products is available online at *www.remss.com*. The data are provided at a resolution of $0.25^\circ \times 0.25^\circ$ grid and averaged up to the common $1^\circ \times 1^\circ$ grid for analysis. Daily mean fields of each parameter are constructed from an average of data from both daytime ($\sim$ 13:30 LST) and nighttime ($\sim$ 01:30 LST) overpasses.

2.2 Quikscat

Surface wind vector data are from the SeaWinds 13.4 GHz microwave scatterometer on the NASA Quikbird sun-synchronous platform. The local overpass times for Quikbird ($\sim$06:00 and 18:00 LST) and we average both passes to provide a daily field. The SeaWinds instrument measures backscatter from wind-driven capillary waves at a number of viewing angles allowing estimates to be made of wind speed and direction with approximately 25 km horizontal resolution. In this study we use the products generated by Remote Sensing Systems using the algorithm of Wentz and Smith

(1999) (url: *www.remss.com*). The swath width guarantees almost complete daily coverage in the regions studied. The data are provided at a resolution of 0.25°×0.25° grid and averaged up to the common 1°×1° grid for analysis.

2.3 Compositing

To locate the cyclones we use a surface pressure anomaly p_0' derived by removal from the daily p_0 field of the sliding window monthly mean surface pressure $\langle p_0 \rangle$. From the (p_0') field we derive first and second order derivatives that are thresholded to obtain candidate gridpoints to represent the cyclone center. These candidates were then filtered to locate the maximum negative anomaly within a 2000 km radius with a p_0 <1015 hPa. Therefore a single cyclone throughout its evolution could be identified as separate systems on consecutive days. From the global analysis of cyclone locations we focus the analysis in this paper upon four subregions: North Pacific (30-55°N, 145°E-165°W); North Atlantic (30-60°N, 10-50°W); South Pacific (30-55°S, 120-180°W); South Atlantic (30-55°S, 50°W-10°E). Cyclone centers must be located within these domains to be considered for analysis.

For each cyclone the satellite fields (initially all on a $1° \times 1°$ grid) are translated and regridded using bilinear interpolation onto a 4000 by 4000 km domain (x, y are the eastward and northward coordinates respectively) with 100 km grid spacing and the cyclone located centrally ($x = 0, y = 0$).

We have examined cyclone properties as a function of cyclone strength and atmospheric moisture metrics that are defined as follows. *Cyclone strength*, $\langle V \rangle$, is determined as the mean surface wind speed, measured using Quikscat, within a circle of radius 2000 km centered on the cyclone. Typically, the central pressure anomaly is used to define the cyclone strength. There are two reasons for preferring $\langle V \rangle$ as an indicator of cyclone strength. First, using observed wind speed minimizes our dependence upon reanalyses. Second, we will show later that a warm conveyor belt model suggests that $\langle V \rangle$ is a more natural indicator of cyclone strength from a cloud and precipitation perspective.

Our atmospheric *cyclone moisture* metric, $\langle WVP \rangle$, is similarly defined as the mean AMSR water vapor path within a circle of radius 2000 km centered on the cyclone. We choose a measure of the atmospheric moisture content as an additional metric because of its importance in cloud and precipitation processes.

In this analysis we conditionally sample the cyclones based on the strength and moisture metrics by binning in terms of $\langle V \rangle$ and $\langle WVP \rangle$. We find that cyclones in the southern hemisphere are similar to their northern hemisphere counterparts for *similar cyclone strength and atmospheric moisture*. We therefore reflect the southern hemisphere cyclones about a zonal axis ($x \rightarrow x, y \rightarrow -y$) and combine all of the cyclones to give a complete database of ∼1300 cyclones with a northern hemisphere sense. Conditional sampling of the cyclones into three moisture categories ($\langle WVP \rangle$: 10-18,18-21,21-33 kg m^{-2}) and three strength categories ($\langle V \rangle$: 4.9-6.95, 6.95-8.14, 8.14-12.3 m s^{-1}) produces nine composite categories each containing at least 69 members.

See Field and Wood (2006) for more extensive information concerning the compositing methodology and data sources used.

3. Results and Discussion

It is clear that rain rates increase with both cyclone strength and moisture (Fig. 1). It is interesting to note that the composite with the deepest low (bottom right panel, central $p_0 < 994$ hPa) does not produce the most rain. In the three cyclone composites with the greatest moisture content the region of high rain rates (> 5 mm day^{-1}) is located close to the cyclone center, but extends out into a 'comma' shape to the east of the cyclone center as the cyclones intensify and eventually wrap around the low center to give a hook-like appearance in the strongest cases.

We consider a simple precipitation model to compare with the observations. The intention is to not supplant what can be accomplished with detailed microphysical modeling, but to provide a simple framework for understanding the variation of the composited rain rates with respect to cyclone strength and atmospheric moisture.

We can explain the observed changes in the composite mean rain rate using an argument based on a simple analytical warm conveyor belt (WCB) model described by Harrold (1973) and Carlson (1998). It is assumed that all of the moisture transported along and up the WCB is rained out. The rate of water mass loaded onto the WCB is $M_{wcb} = \rho_0 q_0 V_{bl} h_{bl} w_{wcb}$ where ρ_0 and q_0 are the air density and water vapor mixing ratio respectively in the planetary boundary layer (PBL) where the WCB originates, V_{bl} is the wind speed in the PBL, h_{bl} is the depth of the boundary layer (that contains most of the moisture) and w_{wcb} is the width of the conveyor belt. To convert M_{wcb} to a rain rate we simply divide by the area over which

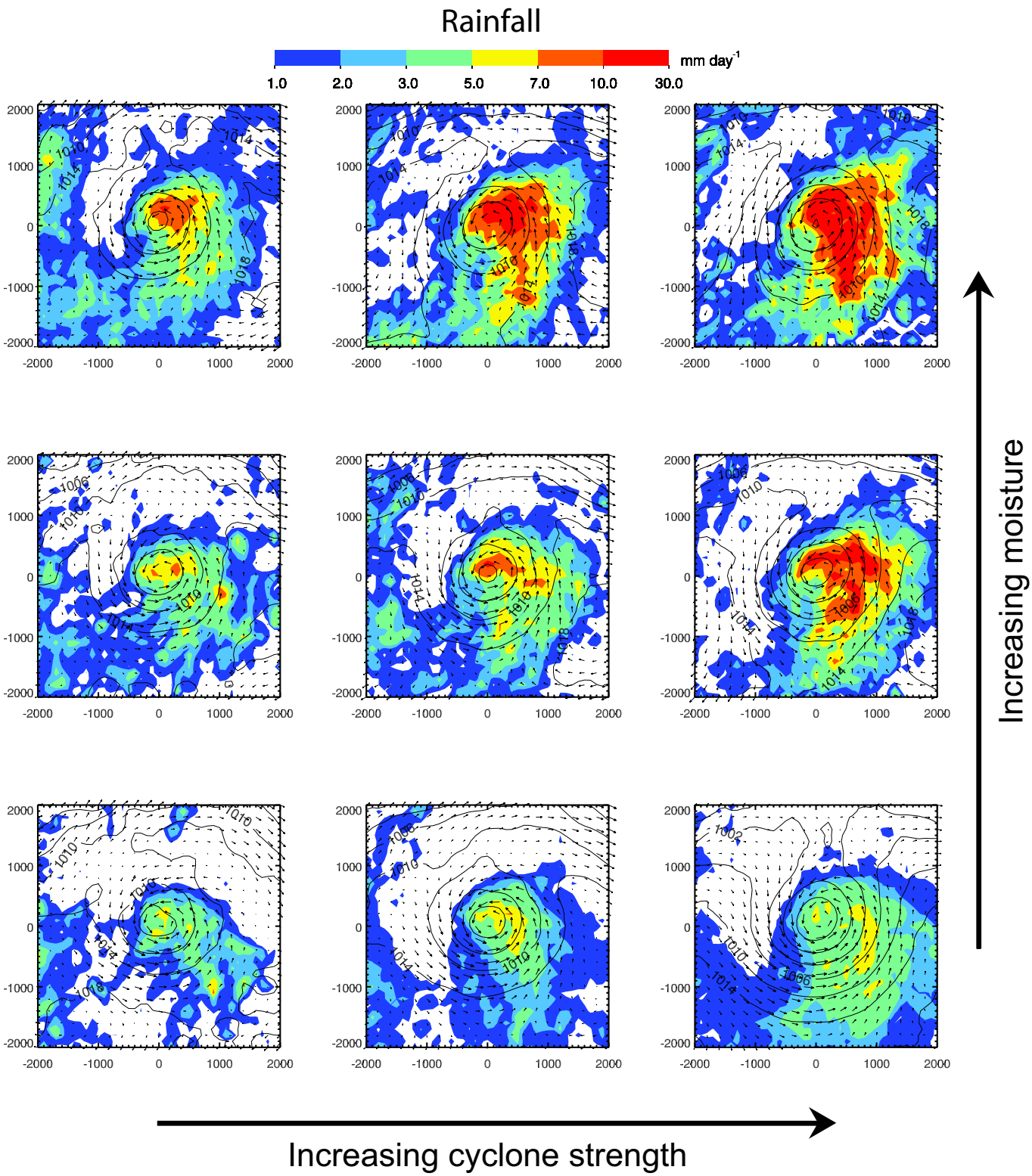

Figure 1: Composites of rain rate for the cyclones from all four regions jointly conditioned on cyclone strength $\langle V \rangle$ (left to right panels) and atmospheric moisture $\langle WVP \rangle$ (lower to upper panels). The categories are $\langle V \rangle$: 4.9-6.95, 6.95-8.14, 8.14-12.3 m s^{-1} and $\langle WVP \rangle$: 10-18,18-21,21-33 kg m^{-2}. The composite mean p_0 and surface wind vectors are also shown.

rain falls. The cyclone mean rain rate from the WCB model is $R_{wcb} = \rho_0 q_0 V_{bl} h_{bl} w_{wcb} / A_c$, where A_c is the cyclone area (=π(2000 km)^2). Assuming that $V_{bl} = \langle V \rangle$ where the angled brackets represent the mean over a circle of radius 2000 km located at the center of the domain (see next section), and $\rho_0 q_0 = k \langle WVP \rangle / S$ where S is a water vapor scale height, $h_{bl} = S$, k is a constant that accounts for the fact that the equatorward side of the cyclone is more moist than the mean value, and letting $c = w_{wcb} k / A_c$ gives

$$R_{wcb} = c \langle WVP \rangle \langle V \rangle \quad (1)$$

We note that for this model the controlling variables are within the composite domain, but it may be the case that some of the moist warm air is advected from well outside of the domain and, as a consequence, the implied width of the warm conveyor belt may seem large compared to case study analyses. To some extent this is expected because the warm conveyor belt will be a composite of many cases and so will naturally be broader than in single realizations. While we accept that it is not perfect, we will show that this simple model, controlled by two cyclone-wide averaged metrics, can be used to quantitatively predict with some skill the cyclone-wide averaged rain rate.

The result from the warm conveyor belt model has been plotted in Fig. 2 assuming c =0.016 (R_{wcb} in mm day^{-1} and $\langle WVP \rangle, \langle V \rangle$ are in SI units) . The WCB model can represent with some skill the dependency of cyclone-wide rain rate, and rationalizes the dependency of rain rate upon cyclone moisture $\langle WVP \rangle$ and strength $\langle V \rangle$. Because of the strong dependency of $\langle WVP \rangle$ on $\langle SST \rangle$ we could equally well represent R_{wcb} as a function of $\langle V \rangle$ and $\langle SST \rangle$. The value for c is appropriate for means computed over a circle of radius 2000 km centered on the cyclone. It should be borne in mind that if the radius of the circle over which the averaging is carried out were to be increased we would start to include rain contributions from neighboring systems. If the radius of the circle over which the averaging is carried were reduced we would begin to lose rain associated with the periphery of the system. Perhaps surprisingly, we find that the value of c is quite robust and only increases by $\sim$25% if we halve the radius of the circle over which the means are computed.

The WCB model can also be used to attempt to understand seasonal variations seen in composite means of rain rate (Chang and Song 2006). In fig. 2 we have overplotted points that represent each season (northern hemisphere winter: December, January, February, southern hemisphere winter: June, July , August, etc) from the cyclone dataset (using all $\sim$1500 cyclones) for all regions. The good agreement with the WCB model leads us to suggest that the seasonal variation seen in rain rate composites can be explained by observed variation in mean cyclone strength and moisture. The out of phase annual variation in the mean values of cyclone strength and moisture combine to produce the maximum mean rain rate in the fall and minimum mean rain rate in the spring.

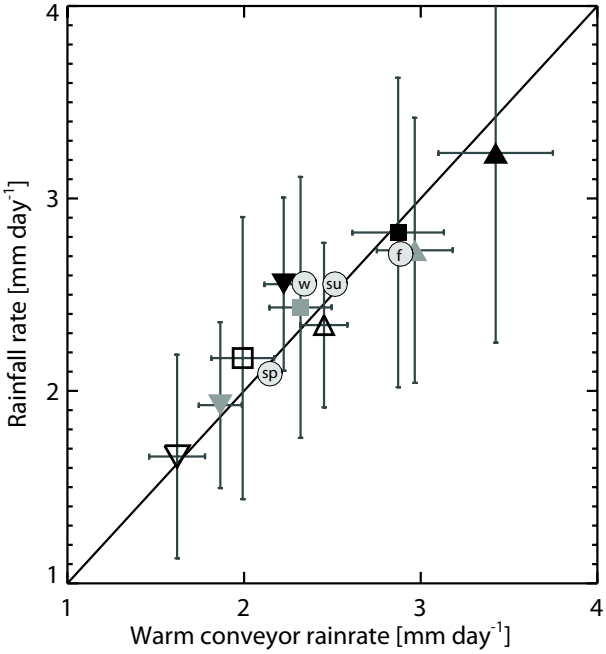

Figure 2: Mean cyclone composite values within a 2000 km circle located at the domain center. The errorbars represent twice the estimate standard error for the mean value. Cyclone strength: open symbols=weak, grey symbols=medium, solid symbols=strong. Cyclone moisture: downward triangles=dry, squares=medium, upward triangles=moist. Cyclone mean rain rate is plotted against rain rate derived from combining cyclone strength and atmospheric moisture with a moist warm conveyor belt argument. The circles represent the results from seasonal composites: w=winter, sp=spring, su=summer, f=fall.

6. REFERENCES

Bjerknes, J.: 1919, On the structure of moving cyclones. *Mon. Weather Rev.*, **47**, 95-99.

Carlson, T. N.:1998, Mid-latitude weather systems. American Meteorological Society, pp507.

Chang, E. K. M. and Song, S. W. : 2006, The seasonal cycles in the distribution of precipitation around cyclones in the western North Pacific and Atlantic *J. Atmos. Sci.*, 63 (3): 815-839.

Field P.R. and Wood R., 2006: Precipitation and cloud structure in midlatitude cyclones. Submitted to J. Clim.

Harrold, T. W., 1990: Mechanisms influencing the distribution of precipitation within baroclinic disturbances. *Quart. J. Roy. Meteorol. Soc.*, **99**, 232-251.

Norris, J.R. and Iacobellis, S.F., 2005: North Pacific cloud feedbacks inferred from synoptic-scale dynamic and thermodynamic relationships *J. Clim.* , 18 (22): 4862-4878.

Shapiro, M. A. and Gronas, S., 1999: The life cycle of extratropical cyclones. Amer. Meteor. Soc.

Wentz, F. J.: 1997, A well calibrated ocean algorithm for special sensor microwave/imager. *J. Geophys. Res.*, **102**, 8703–8718.

Wentz, F. J. and Spencer, R. W.: 1998, SSM/I rain retrievals within a unified all-weather ocean algorithm. *J. Atmos. Sci.*, **55**, 1613-1627.

Wentz, F. J. and D. K. Smith: 1999, A model function for the ocean normalized radar cross section at 14 GHz derived from NSCAT observations. *J. Geophys. Res.*, **104**, 11499–11514.